THE FLYBY ANOMALY: AN INVESTIGATION INTO POTENTIAL CAUSES

B. Jouannic[(1)]**, R. Noomen**[(2)]**, and J.A.A. van den IJssel**[(3)]

[(1)]*Delft University of Technology, Faculty of Aerospace Engineering, Kluyverweg 1, 2629HS Delft, the Netherlands, bjouannic@outlook.com*

[(2)]*Delft University of Technology, Faculty of Aerospace Engineering, Kluyverweg 1, 2629HS Delft, the Netherlands, +31152785377, r.noomen@tudelft.nl*

[(3)]*Delft University of Technology, Faculty of Aerospace Engineering, Kluyverweg 1, 2629HS Delft, the Netherlands, +31152789415, j.a.a.vandenijssel@tudelft.nl*

Abstract: *Since December 1990, a number of spacecraft have performed a flyby around Earth in which an unexpected change in velocity has been observed, which has not been explained so far: the so-called flyby anomaly. The effect on the excess velocity has been expressed in an empirical relation by Anderson, which was based on data on 6 such flybys. However, new flybys did not fit this expression anymore. This paper has made a statistical analysis on a total of 12 flybys (not all of them showing such an anomaly), which has resulted in an improved empirical relation. In addition, the study has investigated a number of physical candidate explanations. Atmospheric drag was rejected as a potential cause, whereas direct solar radiation pressure is a possible candidate, either expressed as an overall coefficient C_R or effectuated by (small) changes in reflectivity coefficients. However, because of lack of data (tracking data, attitude information) no firm conclusions can be drawn.*

Keywords: *Flyby, Anomaly, Astrodynamics, Solar Radiation Pressure.*

1   Introduction

Gravity assist maneuvers around planets are typically used to have an interplanetary spacecraft gain energy. However, such a maneuver around Earth, performed by the Galileo spacecraft in 1990, exhibited a small, but still unexplained difference between prediction and reality: the energy increase of the spacecraft was surprisingly higher than expected. In fact, the post-fit residuals of the tracking data during the flyby showed a strange discontinuity at the time of closest approach: Fig. 1. If we assume the estimation and the modeling of the spacecraft trajectory to be perfect, the residuals should remain about zero throughout the encounter. Here, the amplitude of the discontinuity is around 60 mHz, which corresponds to an instantaneous velocity change at perigee of 2.56 mm/s. Since then, other spacecraft have experienced a similar discrepancy. This phenomenon was named "the flyby anomaly" and is now considered as a major unsolved problem in orbital mechanics. A summary of all relevant Earth flybys is given in Tab. 1. It is clear that not all flybys create such an anomaly; flybys that have taken place since mid-2005 appear to behave as expected.

1.1   Heritage: Investigated Causes

As the flyby anomaly was first detected about 25 years ago, several attempts have been made since to explain this mysterious phenomenon. A few months after NEAR's Earth's passage, a paper was published [1], in which various disturbing forces were dismissed as cause of the observed anomaly: the third-body effect induced by Moon or other planets of the solar system, Earth's oblateness,
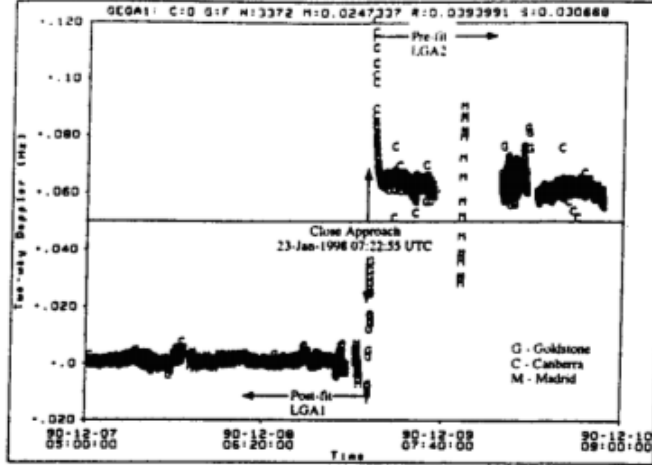
Figure 1: Two-way S-Band Doppler range-rate residuals during Galileo's first Earth gravity assist (December 1990) [1].

Earth's ocean tides and Earth's gravitational field. Iorio [8] investigated general relativity as a possible cause. However, this was discarded since its effect (magnitude 10^{-5} mm/s) is many orders lower than the anomalous ΔV_∞ observed. Adler [9], [10] studied the interaction with a dark matter halo around Earth. It turned out that this phenomenon would not be consistent with the actual trajectories of Earth orbiting satellites. McCulloch tried to explain the flyby anomaly with a theory called modification of inertia due to a Hubble-scale Casimir effect (MiHsC) [11]. In essence, this theory involved a violation of the equivalence principle: $m_{inertial}$ would not be equal to $m_{gravitational}$. However, there is no scientific evidence that there is a difference between the inertial and gravitational mass so far [12]. In conclusion, no physical phenomenon has been identified that could explain the observed flyby anomaly.

1.2 Heritage: Empirical Formulation

In the absence of a physical explanation, Anderson managed to design an empirical formula that accurately describes the magnitude of the anomaly observed during the flybys of Galileo, NEAR, Cassini, Rosetta and Messenger [3]. Although empirical, this formula turned out to give a fair estimate for the anomaly:

$$\frac{\Delta V_\infty}{V_\infty} = K(\cos\delta_{in} - \cos\delta_{out}) \tag{1}$$

where $K = 2\omega_e R_e/c = 3.099 \times 10^{-6}$ and δ_{in} and δ_{out} are the declinations of the incoming and outgoing asymptotic velocity vectors, respectively; ω_e and R_e are Earth's angular velocity and radius, respectively; c is the speed of light.

A comparison between the observed anomalies and Anderson's empirical relation will be made in the next section. Anderson's equation accurately predicts the flybys that were included in its derivation, but the later flybys (two extra Rosetta flybys, three EPOXY flybys and a Juno flyby) are less well predicted (cf. Tab. 1). Obviously, more research is needed to (try to) explain the anomaly.

Table 1: Anomalous ΔV detected during Earth flybys. ΔV_p indicates excess velocity at closest approach and ΔV_∞ the asymptotic excess velocity, h_p denotes height at closest approach, while δ_{in} and δ_{out} represent the declination on the incoming and outgoing asymptotes, respectively. Compiled from [2], [3], [4], [5], [6] and [7].

Spacecraft	Fly-by date	ΔV_p [mm/s]	$\sigma\Delta V_p$ [mm/s]	ΔV_∞ [mm/s]	$\sigma\Delta V_\infty$ [mm/s]	h_p [km]	δ_{in} [deg]	δ_{out} [deg]
GL-I	Dec 1990	2.56	0.02	3.92	0.03	960	-12.52	-34.15
GL-II	Dec 1992	-2.9	0.7	-4.6	1	303	-34.26	-4.87
NEAR	Jan 1998	7.21	0.006	13.46	0.01	539	-20.76	-71.96
Cassini	Aug 1999	-0.42	0.42	-0.5	0.5	1175	-12.92	-4.99
RSTA-I	Mar 2005	0.66	0.011	1.80	0.03	1955	-2.81	-34.29
MGER	Aug 2005	0.0071	0.004	0.02	0.01	2347	31.44	-31.92
RSTA-II	Nov 2007			0	0.1	5301	-10.80	18.60
EPOXI-I	Dec 2007			0	0.1	15614	-5.18	16.90
EPOXI-II	Dec 2008			0	0.1	43415	17.03	64.12
RSTA-III	Nov 2009			0	0.1	2480	18.49	24.37
EPOXI-III	Dec 2009			0	0.1	30404	-63.88	-8.04
Juno	Oct 2013			$\sim$0	n/a	561	14.17	39.50

1.3   This Study

Here we pursue two different approaches. First, a statistical study is carried out, in which the correlation between the observed anomaly and a number of flyby parameters is computed. Anderson only had information for the period 1990-2005 whereas we can extend the interval to 1990-2013. This enables one to freshly determine which parameters appear related to the anomaly. Based on this, a modification of the original empirical formula has been derived, which is able to describe previous and current flybys with and without an anomaly.

Second, as mentioned before, the anomaly can be interpreted as an unexplained ΔV at perigee. The sensitivity of this ΔV_p with respect to various parameters is assessed for each flyby maneuver. In particular, we focus on the anomaly observed for NEAR, because it is the largest one seen so far, and on the ones observed during the two flybys of Galileo, since this is the only possibility to observe the phenomenon on a single vehicle twice. From this sensitivity analysis, it appears that uncertainties of specific satellite parameter values related to direct solar radiation pressure modeling could account for the observed anomalies. In particular, this holds for the reflectivity coefficients of the satellite surface materials.

2   Statistical Analysis

To determine which elements play a role in the flyby anomaly, we assess the correlation between the anomalous ΔV_∞ and different parameters of the corresponding Earth flybys.

2.1 Correlation

The correlation between ΔV_∞ and different parameters is computed using the Pearson product-moment correlation coefficient r for each pair (ΔV_∞, parameter). If the absolute value of Pearson's coefficient becomes closer to one, the relationship between the two variables is more linear [13]. In addition, a parameter might have an influence on the magnitude of the anomaly, while not being able to rule its sign. Therefore, all correlation calculations are done twice, once using the value of the flyby anomaly as is, and a second time using the absolute value of the anomaly. Usually, $r > 0.5$ is considered an indication that two variables are correlated. However, there can be large differences between data sets leading to the same value of r [14]. For all considered parameters, we have therefore also graphically plotted the data along a regression line for visual inspection. These plots are available in [15].

2.2 Data Used

In order to carry out the correlation analysis, a wide range of parameters that play part in a flyby has been selected. The values of most of these parameters were obtained from the JPL Horizon database [16] or derived using these values [15]. The Earth's magnetic field strength at closest approach was computed using the International Geomagnetic Reference Field [17], while the international sunspot number is provided by the Solar Influences Data Analysis Center [18]. Minimum and maximum satellite cross-sectional areas were derived from technical satellite drawings available at NASA and ESA [19] [20].

2.3 Results

In total, 27 flyby parameters have been selected for the correlation analysis. Tab. 2 gives an overview of the resulting correlation coefficients. The first column presents the correlation coefficient between the flyby parameter and ΔV_∞, while the second column shows the correlation between the flyby parameter and the absolute value $|\Delta V_\infty|$. Although not included here, we also calculated the correlation between ΔV_∞ and the cosine/sine/tangent/inverse of any angular flyby parameter.

From Tab. 2, one can see that several parameters correlate significantly with ΔV_∞. The high correlation coefficient for *Time spent below 2000 km altitude* (0.72) indicates that the observed anomaly could be related to something that occurs close to Earth. Possible candidates are Earth's atmosphere (atmospheric drag) and magnetosphere (Lorentz force). Other parameters that could support the hypothesis that the anomaly is provoked by atmospheric drag are the maximum cross-sectional area and mass of the spacecraft. These parameters show relatively small correlations of, respectively, 0.26 and 0.23. The correlation between the anomaly and the strength of Earth's magnetic field at perigee is slightly larger (0.35), supporting the hypothesis of the Lorenz force.

Although not shown here, the inverse of the altitude shows a significant correlation coefficient (0.57), which supports atmospheric drag as a likely candidate. In addition, the fact that the anomaly also correlates well with the latitude of perigee (0.46) may again indicate that the anomaly depends on atmospheric drag and/or Earth's magnetic field, as both the atmospheric density and the strength and orientation of the Earth's magnetic field vary with latitude. The correlation with latitude could also

4

Table 2: Correlation *r* between selected flyby parameters and ΔV_∞ (*Value*) or $|\Delta V_\infty|$ (*Absolute value*).

Parameter	Value	Absolute value
Time spent below 2000 km altitude	0.38	0.72
Outgoing Asymptote Declination	0.62	0.69
Julian Day	0.23	0.60
C/A latitude	0.54	0.46
Argument of Periapsis	0.44	0.46
Magnetic field strength at C/A	0.21	0.35
Sun-Earth-S/C angle	0.10	0.32
Altitude	0.17	0.32
Incoming Asymptote Declination	0.06	0.29
Semi-major axis	0.09	0.28
RAAN (ECEF)	0.10	0.27
Max cross section	0.18	0.26
Sunspots Number	0.15	0.25
S/C-Earth-Moon angle	0.01	0.23
Mass	0.30	0.23
Eccentricity	0.22	0.22
Inclination	0.08	0.22
Incoming Asymptote Elevation	0.17	0.19
RAAN (ECI)	0.20	0.18
C/A longitude (ECEF)	0.43	0.18
Deviation angle	0.20	0.14
C/A Local solar time	0.16	0.13
Outgoing Asymptote Elevation	0.03	0.08
Min cross section	0.29	0.08
Perigee/Asymptotic velocity ratio	0.16	0.08
C/A longitude (ECI)	0.02	0.07
Asymptotic velocity	0.10	0.03

indicate that the flyby anomaly might arise from measurement errors due to ionospheric disturbances. The Earth's ionosphere varies strongly with latitude and this can affect the electromagnetic waves used for the Doppler tracking of the spacecraft. However, further analysis showed that the expected measurement error is small, especially when X-band tracking is used [15].

The moderate level of correlation between the anomaly and the sunspot number (0.25) is also interesting, since solar activity plays a role in all proposed potential causes. Solar activity can strongly impact the air density at a given altitude, modify the strength of the Earth's magnetic field and disturb the ionosphere. Tab. 2 also shows that the anomaly correlates well with the Julian Day of the flybys (0.60). This suggests that the flyby anomaly was due to a measurement or data processing error that has been fixed now. More observations and information on the (modeling of the) specific flybys are required to decide whether this is a possible explanation.

As an illustration, the correlation between mass and $|\Delta V_\infty|$ is presented in Fig. 2. Obviously, the lower the mass, the higher is the anomaly. However, there are a few exceptions to this rule and the relationship does not seem to be linear. This explains why the correlation coefficient is quite low (0.23). This suggests that a single parameter is not able to explain the flyby anomaly, which was to be expected, in view of Anderson's empirical expression. Therefore, we have also investigated correlations with different combinations of the selected flyby parameters.
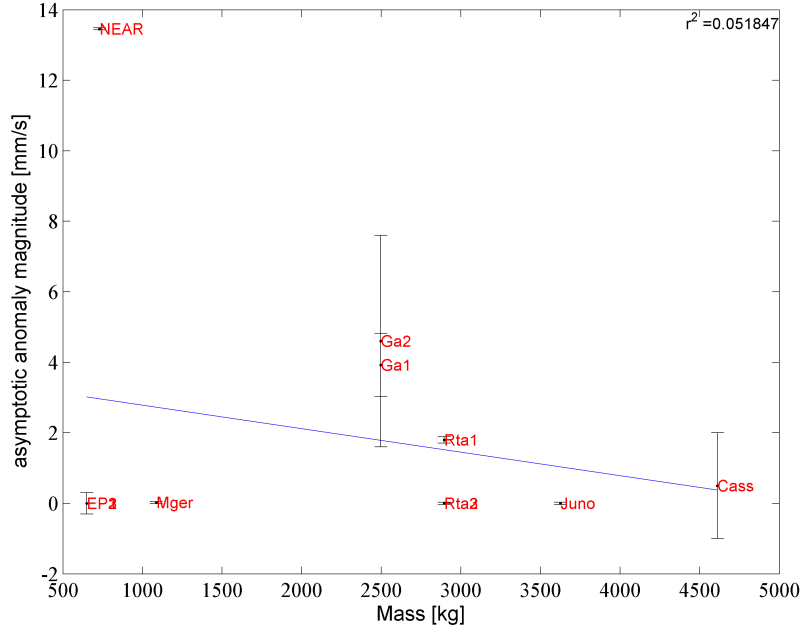
Figure 2: Correlation between the absolute value of the anomaly and mass.

2.4 Improved empirical formula

As previously stated, combinations of parameters give better correlations with the anomaly than individual parameters. The strongest correlation was found for the following combination:

$$\Delta V_\infty = \Lambda V_\infty issn \frac{\cos \delta_{in} - \cos \delta_{out}}{mh} \tag{2}$$

where Λ is an empirically obtained value equal to 30922.11 kg.m (of course, based on all 12 flybys). In addition to the declination of the incoming and outgoing asymptote, which are used in the original empirical formula, the international sunspot number and the inverse of the satellite mass and altitude at closest approach are now also included. With this improved empirical formula, the correlation coefficient r^2 reaches 0.95. If the magnetic field strength B would be included as well, the correlation coefficient would slightly drop to an r^2 value of 0.87.

The results produced by the original and improved empirical formula are compared with the actual observed anomalies in Fig. 3. In addition, Tab. 3 shows correlation values for both formulae based on the old dataset of 6 flybys and the new dataset, which includes 12 flybys. One can see that the original formula of Anderson [3] leads to a high correlation coefficient for the old set of 6 flybys, but for the entire set of 12 flybys the correlation coefficient is significantly reduced. The new formula better predicts the value of the anomaly for the recent flybys (EPOXI and Juno). Compared to the original one, our expression is doing slightly worse for Galileo I and II and Rosetta I, but is able to reproduce the anomaly observed during the NEAR, Cassini, Rosetta II and III and the EPOXI I, II and III flybys much more accurately. The result of our improved formula for Juno is a bit off the observed value, but it is still closer than the value provided by the original one. It will be interesting
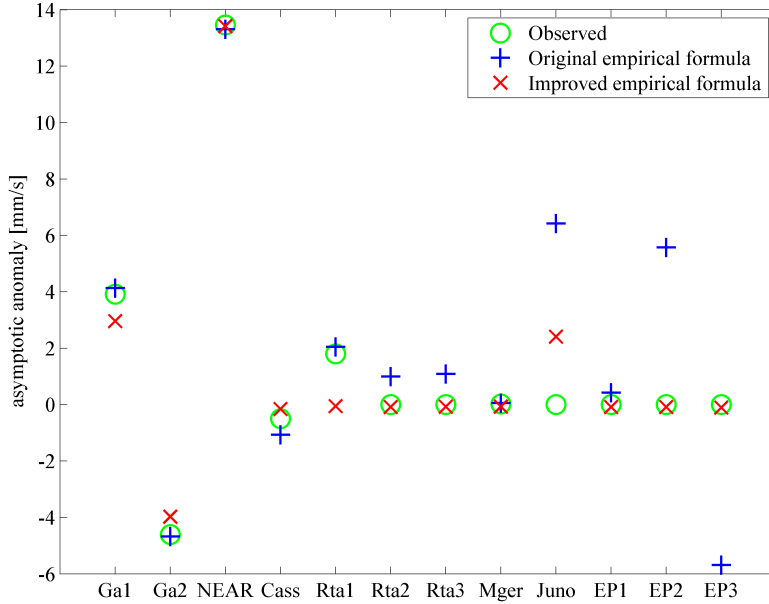
6

Figure 3: Comparison of the original and improved empirical formulae predictions versus the observed anomaly magnitudes.

Table 3: Comparison of the fitting accuracy between Anderson's and our improved empirical formula

Empirical formula	6 flybys		12 flybys	
	r	r^2	r	r^2
Anderson [3]	0.999	0.998	0.804	0.647
This study	0.989	0.977	0.974	0.948

to observe how accurately this formula manages to foresee the anomaly that Hayabusa 2 (December 2015) and BepiColombo (July 2018) may encounter during their respective Earth flybys.

3 Orbit Propagation Analysis

Next, we will investigate whether certain physical phenomena could account for the anomaly. We explain the concept behind our analysis first.

3.1 Concept

The fundamental idea is to compute, by using orbit propagation, a quantity ΔV_p, similar to the value of the observed anomaly, and to investigate how sensitive it is to various parameters of the problem. This ΔV_p is computed as follows: two state vectors of the considered spacecraft (when it enters and leaves the Earth's sphere of influence, respectively) are propagated toward perigee (one forward in time, the other backward). The state vectors are obtained from JPL's Horizon ephemeris system [16],

7

and propagated using NASA's GEODYN II software [21]. For both propagations the subsequent velocity at perigee is then computed, which, subtracted, gives a velocity difference at perigee. The integration was done with a Cowell 11th-order integrator, which is standard available in GEODYN II. A step-size of 1 sec was selected. This gives an accuracy of the velocity difference at perigee of 0.2 mm/s or better, and provides a velocity close to perigee (no interpolation is needed).

Obviously, the value for ΔV_p obtained here is not necessarily identical to the observed anomalies (although in the same range), the reason for this being subtle differences in our modeling and that of the original evaluations which lead to the acclaimed anomaly values. However, when repeated with different values for a range of propagation parameters, it gives a direct quantification of the sensitivity to the particular parameter in our model. We varied the following input parameters: (i) spacecraft attitude, (ii) spacecraft drag coefficient C_D, (iii) spacecraft solar radiation pressure coefficient C_R, and (iv) reflectivity coefficients of the materials covering the spacecraft. The attitude of the spacecraft is amongst the elements to be varied. This is due to the fact that no information is publicly available about the attitude of any of the spacecraft.

The reason why we are interested in the sensitivity of the anomaly with respect to the aforementioned parameters (other than attitude) is that each one has a non-negligible uncertainty. In fact, their actual value may deviate from what was considered as their nominal one for the computation that revealed the anomaly. Our study then assesses whether a reasonable change in any of these parameters could account for the anomaly. It is important to notice that we are only interested in this *sensitivity* of ΔV_p with respect to several parameters, which means that the absolute value of the anomaly is of limited importance in our setup. We define *sensitivity* being the derivative of ΔV_p with respect to a given parameter: $s(X) = \partial (\Delta V_p)/\partial (X)$, where X represents an arbitrary parameter of interest. Assuming that ΔV_p behaves linearly with respect to X, we can compute the change in X, ΔX, required to account for the observed anomaly. Finally, based on the value of ΔX we can argue whether the considered parameter could explain the anomaly.

As the spacecraft attitude is publicly unavailable, we had to study the sensitivity of the anomaly for a range of possible orientations. We selected a total of 12 different attitudes, which are constructed using two different right-handed frames of reference: one Earth-pointing and another Sun-pointing. The Earth-pointing frame is characterized as follows: Z-axis in nadir direction, Y-axis in flight direction, and X-axis in cross-track direction. The Sun-pointing frame is defined by: Z-axis in nadir direction, Y-axis perpendicular to both the Sun-satellite vector and the Z-axis, and X-axis in the direction toward the half plane that contains the Sun. So, both reference frames have the same Z-axis, but their respective X- and Y-axis are generally different. For these two reference frames, we considered all six possible orientations of the satellite body-fixed frame. This means that the satellite body-fixed X-axis is either aligned along the ± X-, Y- or Z-axis of the considered Earth-pointing or Sun-pointing frame, leading to a total of 12 different considered attitudes.

3.2 Selected spacecraft

Two spacecraft were particularly interesting for our study. The first one, NEAR, is the one which exhibited the highest anomaly ever observed and it was thus deemed to be the one that would provide the clearest information about the flyby anomaly. Galileo, the second spacecraft considered,

Table 4: Panel model used for the Galileo spacecraft in the satellite body-fixed frame.

Panel n°	Material	Reflectivity [-]		Area [m²]	$\vec{n}$		
		ρ_s	ρ_d		x	y	z
1	Antenna	0.01	0.07	4.52	1	0	0
2	Probe	0.01	0.8	4.52	-1	0	0
3	Black Kapton	0.01	0.07	9.752	0	0	1
4	Black Kapton	0.01	0.07	9.752	0	0	-1
5	Black Kapton	0.01	0.07	9.752	0	1	0
6	Black Kapton	0.01	0.07	9.752	0	-1	0
7	Black Kapton	0.01	0.07	9.752	0	1	1
8	Black Kapton	0.01	0.07	9.752	0	1	-1
9	Black Kapton	0.01	0.07	9.752	0	-1	1
10	Black Kapton	0.01	0.07	9.752	0	-1	-1

performed two gravity assist maneuvers around Earth, which provided two data points on the anomaly on one and the same vehicle. This reduces uncertainty: for example, it is likely that the surface properties did not change (much), and the attitude of the spacecraft might be more or less the same for the two flybys. Other spacecraft flew by Earth several times but none of them experienced the flyby anomaly more than once (cf. Tab. 1). The body-fixed frames of reference used for NEAR and Galileo are defined in Fig. 4.
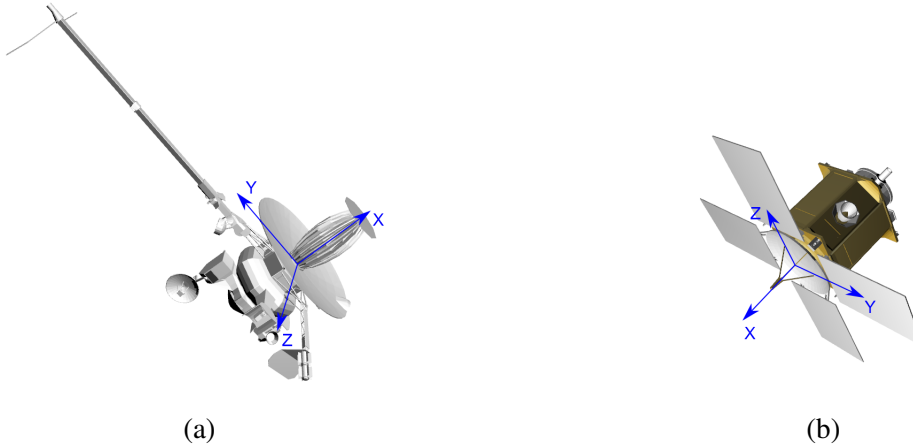

(a)   (b)

Figure 4: Definition of the body-fixed frame of reference of Galileo (a) and NEAR (b) [22].

Panel model

In order to accurately reconstruct the orbit of each satellite from a given state vector, we need to implement a three-dimensional spacecraft model in GEODYN II, the orbit computation software used. To do so, each satellite is modeled with a number of (flat) panels. Obviously, some simplifications have to be made here. For instance, and especially true for Galileo, instruments sticking out are not taken into account, and curved surfaces are approximated with a set of rectangular panels.

Table 5: Panel model used for the NEAR spacecraft in the satellite body-fixed frame.

Panel n^o	Material	Reflectivity [-]		Area [m^2]	$\vec{n}$		
		ρ_s	ρ_d		x	y	z
1	Solar cell	0.01	0.35	8.64	1	0	0
2	Solar panel	0.01	0.168	8.64	-1	0	0
3	Antenna	0.02	0.85	1.77	1	0	0
4	Aft deck	0.014	0.168	2.25	-1	0	0
5	MLI	0.184	0.736	1.951	0	0	1
6	MLI	0.184	0.736	1.951	0	0	-1
7	MLI	0.184	0.736	1.951	0	1	0
8	MLI	0.184	0.736	1.951	0	-1	0
9	MLI	0.184	0.736	1.951	0	1	1
10	MLI	0.184	0.736	1.951	0	1	-1
11	MLI	0.184	0.736	1.951	0	-1	1
12	MLI	0.184	0.736	1.951	0	-1	-1

The panel models developed for Galileo and NEAR are given in, respectively, Tab. 4 and 5. In these tables, the coefficients ρ_s and ρ_d stand for specular and diffuse reflectivity, respectively. Together with the surface area and the orientation, they are the sole parameters used for the characterization of the panel. The nominal value of the drag coefficient C_D is set to 2.3, whereas the solar radiation scaling factor C_R has been set to 1.5 nominally. Very little information is available in literature about the surface properties of Galileo and NEAR. Instead, we used values of similar materials employed on other spacecraft (ERS-2, CHAMP, SWARM and TOPEX/POSEIDON). Approximate values for the surface area and orientation of each panel are determined based on technical drawings of the satellite available at NASA [23].

4 Sensitivity results

The sensitivity of the anomalous velocity change at perigee ΔV_p is assessed with respect to three parameters: atmospheric drag force, solar radiation pressure force and surface properties of the spacecraft. For each of these parameters, 12 different spacecraft attitudes are considered, to account for the uncertainty in the satellite attitude.

4.1 Atmospheric drag

The statistical analysis, presented in Section 2, suggested that atmospheric drag is a likely candidate to explain the flyby anomaly. Therefore we have tested if it is possible that uncertainties in the parameters used to determine the atmospheric drag acceleration could lead to the observed velocity change during the satellite flyby. We only studied the sensitivity of ΔV_p with respect to C_D, as a change in the value of this coefficient can be interpreted as the net effect of changes in various elements of the drag formulation, like atmospheric density, effective cross-sectional area, mass and C_D itself.

As explained in Section 3.1, we first computed for each attitude the value of the sensitivity $s(C_D)$, and then converted this to the required change in C_D that is needed to explain the anomaly. For the flyby of NEAR and the two flybys of Galileo, the required changes in C_D would be in the order of 1000, 0.5 and 100, respectively. Clearly, such modifications (as in errors in the computations by NASA and ESA) are unrealistic. Therefore, atmospheric drag has to be discarded as a mechanism for explaining the observed anomalies.

4.2 Radiation pressure

Definition

An alternative perturbing acceleration that is also mass-related is solar radiation pressure. It arises from the momentum transfer that occurs when photons of light impinge on the surface of a spacecraft. The corresponding acceleration is formulated as [21]:

$$\vec{a}_{Solar} = \nu C_R \frac{1}{m} \sum_{j=0}^{n} \vec{F}_j^{sun} \tag{3}$$

with $\vec{F}_j^{sun}$ the solar radiation force acting on the jth panel:

$$\vec{F}_j^{sun} = \left[2\rho_{s,j} \cos^2 \theta_j + \rho_{d,j} \frac{2}{3} \cos \theta_j \right] A_j \frac{\Phi_0}{c} \left(\frac{a_{sun}}{r_{sun}} \right)^2 \hat{u}_{n,j} + (1 - \rho_{s,j}) \frac{\Phi_0}{c} A_j \cos \theta_j \left(\frac{a_{sun}}{r_{sun}} \right)^2 \hat{u}_{i,j} \tag{4}$$

where ν is the eclipse factor (0 or 1), C_R is the solar radiation pressure scaling coefficient and A_j the area of panel j. C_R is an overall factor that not only reflects the momentum transfer of incoming photons, but also the effective pressure of reflected photons. It allows for the adjustment of the net acceleration in case of modeling errors in *e.g.* mass and area of the spacecraft. We can also define the terrestrial radiation pressure, which comprises both the albedo and the infrared radiation of Earth in a similar fashion, but now with index *earth* instead of *sun*.

Influence of terrestrial radiation pressure

First we assessed the influence of Earth's radiation: do reflected sunlight and Earth thermal radiation play a significant role? To that end, the value of ΔV_p was computed for each attitude and flyby, with and without taking terrestrial radiation into account. The maximum value for ΔV_p obtained for any satellite or configuration was 0.015 mm/s^2. Clearly, this type of radiation cannot be held responsible for the flyby anomaly. There is a side-effect of this: it suffices to concentrate on direct solar radiation only. In other words: the values for all coefficients ρ_s and ρ_d are to be taken for the visible part of the spectrum.

Influence of solar radiation pressure

Similar as for atmospheric drag, the sensitivity of ΔV_p with respect to C_R was computed. Based on this value the required change in C_R was determined that is needed to explain the anomaly. The results are shown in Tab. 6. Interestingly, for the two flybys of Galileo, the ΔC_R required to account

for the anomaly is rather small for most configurations, and shows a certain consistency between the two flybys, with results that differ by "only" a factor two. Taking into account that the required ΔC_R is with respect to the nominal value of 1.5, it is clear that an error of only a few percent in the modeling of the acceleration caused by solar radiation pressure could produce the observed anomaly. Concerning NEAR, a greater ΔC_R is required, for some cases it is even unrealistically large. This is especially true for both Sun and Earth pointing attitude when the spacecraft antenna is oriented along the $+Z$ or $-Z$ axis. These cases correspond to configurations for which the influence of solar radiation pressure is slight (small value for $s(C_R)$), and thus a large ΔC_R is required to account for the anomaly. However, there are still a number of configurations where the amount of error required to eliminate the anomaly is between 10 and 25%. Such errors are nonetheless reasonable, since there are multiple sources of potential error (mainly cross-sectional area, mass and reflectivity coefficients) that can add up.

Table 6: Required change in C_R to account for the flyby anomaly of Galileo and NEAR, assuming different attitude configurations.

Attitude	ΔC_R (Galileo I)	ΔC_R (Galileo II)	ΔC_R (NEAR)
Earth pointing			
$+X$	0.019	0.029	0.31
$-X$	0.019	0.029	0.33
$+Y$	0.017	0.068	0.15
$-Y$	0.013	0.022	0.23
$+Z$	0.018	0.029	81.90
$-Z$	0.018	0.030	2.69
Sun pointing			
$+X$	0.017	0.052	0.25
$-X$	0.013	0.034	0.25
$+Y$	0.019	0.033	0.55
$-Y$	0.019	0.033	0.55
$+Z$	0.018	0.033	2.63
$-Z$	0.018	0.032	149.28

Modification of reflectivity coefficients

The most uncertain elements in the radiation acceleration expression are certainly the reflectivity coefficients, for two main reasons. First, the values of these coefficients for the surface materials of Galileo and NEAR are nowhere to be found in literature, making it well possible that their specific values were not precisely assessed before launch. Secondly, both vehicles spent several years in space before performing their flyby(s). Having been exposed to the harsh outer space environment so long, the surface properties of any material, and especially its reflectivity, may have changed significantly. For instance, the reflectance of white paint (S13GLO) in the visible wavelength can easily drop from 0.82 to 0.3 over a period of 6 years [24].

For these reasons, we decided to study the influence of the reflectivities of each material on ΔV_p. We followed again the same approach: the sensitivity of ΔV_p with respect to each coefficient was computed for each satellite and every configuration. The sensitivities $s(\rho_{s,mat_i})$ and $s(\rho_{d,mat_i})$ are

defined as $s(\rho_{s,mat_i}) = \partial\Delta V_p / \partial\rho_{s,mat_i}$ and $s(\rho_{d,mat_i}) = \partial\Delta V_p / \partial\rho_{d,mat_i}$, where the subscript mat_i represents a given type of material, like MLI or solar cell. While calculating these derivatives for each attitude/spacecraft configuration for a particular component, the reflectivity coefficients of the other materials (mat_2, mat_3...) were kept fixed at their nominal value. As a result, we obtained the values of $s(\rho_s)$ and $s(\rho_d)$ for each material and for every attitude configuration. To make the problem manageable, we assumed that the sensitivities of each material are independent of the values of the reflection coefficients of any other material. This is very reasonable, since, for instance, for the Galileo spacecraft the sensitivity of ρ_s of the antenna material changed from -36.261 to -36.269 mm/s^2 when the value of ρ_s for black Kapton was set successively to 0.01 and 0.1.

Since in principle we can change all coefficients simultaneously, there is an infinite number of combinations that would, in the end, produce the observed anomaly. To make a selection and obtain the most realistic results, we designed a mathematical formulation of our problem that provides a unique solution per attitude. The main assumption is that the combination which requires the minimal deviation of the coefficients from their nominal value is most realistic. Therefore, we have an optimization problem defined by the following set of equations.

The function f to be minimized is:

$$f = \frac{1}{n}\sum_i (\Delta\rho_{s,\mathrm{mat}_i})^2 + \frac{1}{n}\sum_j (\Delta\rho_{d,\mathrm{mat}_j})^2 \tag{5}$$

where $\Delta\rho$ is the difference between the nominal and the modified value of the coefficient.

The minimization has to satisfy several constraints. First and foremost, the resulting variation of ΔV_p has to equal the observed anomaly, which translates into:

$$\sum_i \frac{\partial\Delta V_p}{\partial\rho_{s,\mathrm{mat}_i}}\Delta\rho_{s,\mathrm{mat}_i} + \sum_j \frac{\partial\Delta V_p}{\partial\rho_{d,\mathrm{mat}_j}}\Delta\rho_{d,\mathrm{mat}_j} = \Delta V_p \tag{6}$$

In addition, any reflectivity coefficient is always positive and has a value between zero and one.

For each case, one can derive, using Lagrange multipliers and Karush-Kuhn-Tucker conditions, whether this constrained minimization admits a solution. When existing, the solution was computed and the corresponding results are shown in Tab. 7, 8 and 9. These tables provide the required change of each reflectivity coefficient to account for the flyby anomaly. There are configurations for which the modification of a given coefficient has no or little impact on the value of ΔV_p; these cases are denoted by the dash symbol. One may also notice that in the case of NEAR (Tab. 9), only two attitudes are shown. For other attitudes, it was not possible to satisfy all constraints at the same time; *e.g.* some coefficients would become larger than one to reproduce the anomaly, which is physically impossible.

From the results given in Tab. 7, 8 and 9, we can conclude that the modification of the reflectivity coefficients successfully reproduced the anomalous velocity change at perigee observed in the Galileo and NEAR flybys. The required modifications are small and typically range from 10^{-4} to

Table 7: Required change in specular and diffuse reflectivity coefficients to produce a ΔV_p change that equals the anomaly observed during the first flyby of Galileo.

	Antenna		Black Kapton		Probe		RMS
	$\Delta\rho_s$	$\Delta\rho_d$	$\Delta\rho_s$	$\Delta\rho_d$	$\Delta\rho_s$	$\Delta\rho_d$	
Earth pointing							
$+X$	-0.002	0.0001	0.0194	-0.0321	-	-	0.0188
$-X$	-	-	-	-0.387	0.0024	-0.0001	0.0224
$+Y$	-0.0066	-0.0104	0.0178	-0.0009	-	-	0.0108
$-Y$	-	-	0.0178	-0.009	-0.0066	-0.0105	0.0108
$+Z$	0.0180	-0.0008	-0.0059	-0.0231	0.0081	-0.0007	0.0126
$-Z$	0.0081	-0.0007	-0.0059	-0.0231	0.0180	-0.0008	0.0126
Sun pointing							
$+X$	-0.0069	-0.0107	0.0178	-0.0008	-	-	0.0109
$-X$	-	-	0.0178	-0.0008	-0.0069	-0.0107	0.0109
$+Y$	-	-	-	-0.0387	-	-	0.0387
$-Y$	-	-	-	-0.0387	-	-	0.0387
$+Z$	0.0081	-0.0007	-0.0066	-0.0229	0.0177	-0.0009	0.0126
$-Z$	0.0177	-0.0009	-0.0066	-0.0229	0.0081	-0.0007	0.0126

4×10^{-2}. As for Galileo, there is always (*i.e.* for all 12 attitudes considered) a set of modifications that produces a change in ΔV_p similar to the observed anomaly. Unfortunately, the best scenarios (*i.e.* for which the RMS of the $\Delta\rho$'s is lowest) for the first flyby (Earth-pointing $+Y$ and $-Y$) are not identical to those of the second flyby (Sun-pointing $+Z$ and $-Z$). It is therefore not possible to conclude which attitude is most likely (assuming that the spacecraft attitude was identical during both flybys). For NEAR, there are only two configurations for which the anomaly can be explained by physically acceptable modifications of the reflectivities. In each case, the $\Delta\rho$ required is relatively small. In fact, the RMS of the required changes is always in the order of 10^{-2}, which corresponds to an error of 2% or less in the reflectivity coefficient. Thus, it is reasonable to consider that the flyby anomaly might be caused by errors made in the modeling of those parameters. The reason why the values assumed for these parameters would be different from their real ones is still to be determined. As mentioned earlier in this section, possible explanations are inaccuracies in the measurements of the reflectivity properties conducted before launch and their variation induced by a prolonged exposure to the space environment.

5 Conclusions

The aim of our study was to investigate the potential causes of the mysterious Earth flyby anomaly. We followed a twofold approach: we carried out an empirical statistical analysis, and then we investigated the physical relation between dynamical parameters and the anomalous velocity difference at perigee.

The statistical analysis produced two interesting results. First, one of the (many) regression analyses allowed us to design a new empirical formula, improving the "classical" one by Anderson [3]. Our improved empirical relation presents a higher correlation coefficient with the observational data

Table 8: Required change in specular and diffuse reflectivity coefficients to produce a ΔV_p change that equals the anomaly observed during the second flyby of Galileo.

	Antenna		Black Kapton		Probe		RMS
	$\Delta\rho_s$	$\Delta\rho_d$	$\Delta\rho_s$	$\Delta\rho_d$	$\Delta\rho_s$	$\Delta\rho_d$	
Earth pointing							
$+X$	-	-	0.0267	0.0449	-0.0143	0.0002	0.0271
$-X$	-0.0143	0.0002	0.0267	0.0449	-	-	0.0271
$+Y$	0.0148	0.0103	0.0031	0.0003	-0.0040	-0.0052	0.0079
$-Y$	-0.0040	-0.0052	0.0031	0.0003	0.0148	0.0103	0.0079
$+Z$	-0.0101	0.0003	0.0168	0.0214	0.0249	0.0007	0.0156
$-Z$	0.0248	0.0007	0.0168	0.0214	-0.0101	0.0003	0.0156
Sun pointing							
$+X$	0.0246	0.0120	0.0115	0.0007	-	-	0.0149
$-X$	-	-	0.0115	0.0007	0.0246	0.0120	0.0149
$+Y$	-	-	0.0288	0.0471	-	-	0.0390
$-Y$	-	-	0.0288	0.0471	-	-	0.0390
$+Z$	0.0225	0.0007	0.0189	0.0192	-0.0088	0.0002	0.0148
$-Z$	-0.0088	0.0002	0.0189	0.0192	0.0225	0.0007	0.0148

and provides a better estimation of the anomaly for the recent Earth flybys (*i.e.* EPOXI I and II and Juno) and also for the Cassini, Rosetta II and III flybys. Upcoming flybys of Hayabusa 2 (December 2015) and BepiColombo (July 2018) will put our new empirical relation to the test. Secondly, by reviewing the correlations, we were able to propose several candidate explanations for the flyby anomaly: phenomena that are related to the mass and altitude at closest approach of the considered spacecraft. This could signify that it is caused by a force related either to mass, altitude, or both, like, for instance, atmospheric drag or solar radiation pressure.

In order to study actual orbit behaviour, we designed a panel model for Galileo and NEAR. For NEAR, the model is made of 12 different panels, while Galileo is represented by 10 panels. These models allowed us to study the influence of atmospheric drag and solar radiation pressure on the velocity difference at perigee. Using these models, we ran many orbit simulations for two different attitude configurations (Earth and Sun pointing) and for various orientations of the spacecraft. In each case, input parameters such as C_D, C_R and the reflectivity coefficients ρ of the satellite surface materials were varied in order to quantify the sensitivity of ΔV_p relative to these variables.

From these simulations, we managed to extract a potential solution to the flyby anomaly. We clearly showed that atmospheric drag can not be the cause of the anomaly, since it would require unrealistically large modifications in the drag model. Solar radiation pressure presented more interesting results: small changes in the solar radiation pressure coefficient C_R could explain the anomaly. In more detail, uncertainties in the values of the reflectivity coefficients of the materials that cover the spacecraft could be held responsible for the anomalous velocity change observed. Actually, we proved that modifications of the specular and diffuse reflectivity coefficients by an amount ranging from 10^{-4} to $4\ 10^{-2}$ are sufficient to successfully eliminate the unexpected velocity shift at perigee.

Table 9: Required change in specular and diffuse reflectivity coefficients to produce a ΔV_p change that equals the anomaly observed during the NEAR flyby.

	Element	$\Delta\rho_s$	$\Delta\rho_d$	RMS
Earth pointing				
	Solar cells	-	-0.104	
	Solar panel	-0.033	-0.016	
$+Y$	MLI	0.043	0.102	0.0567
	Antenna	-	-0.021	
	Aft deck	0.011	0.027	
	Solar cells	0.043	0.102	
	Solar panel	-0.033	-0.016	
$-Y$	MLI	-	-0.104	0.0568
	Antenna	0.009	0.021	
	Aft deck	-	-0.027	
Sun pointing				

6 References

[1] P. G. Antreasian and J. R. Guinn. Investigations into the unexpected delta-v increase during the Earth Gravity Assist of GALILEO and NEAR. *AIAA/AAS Astrodynamics Specialist Conf. and Exhibition*, (98-4287), 1998.

[2] John D. Anderson, James K. Campbell, and Michael Martin Nieto. The energy transfer process in planetary flybys. *New Astronomy*, (12), July 2007.

[3] John D. Anderson, James K. Campbell, John E. Ekelund, Jordan Ellis, and James F. Jordan. Anomalous orbital-energy changes observed during spacecraft flybys of Earth. *Physical Review Letters*, (10), March 2008.

[4] T. Morley and F. Budnik. Rosetta navigation at its first Earth swing-by. *Japan Society for Aeronautical and Space Sciences International Symposium on Space Technology and Science*, 2006.

[5] J. D. Anderson and J. K. Campbell. Private email communications, 2013.

[6] ESA-Rosetta. ESA's website dedicated to Rosetta mission. `http://www.esa.int/Our_Activities/Space_Science/Rosetta`, 2015. Accessed: 2015-02-15.

[7] Paul F. Thompson, Matthew Abrahamson, Shadan Ardalan, and John Bordi. Reconstruction of Earth flyby by the Juno spacecraft. *AAS*, (14 - 435), 2014.

[8] Lorenzo Iorio. The effect of general relativity on hyperbolic orbits and its application to the flyby anomaly. *arXiv preprint arXiv:0811.3924*, 2008.

[9] Stephen L Adler. Can the flyby anomaly be attributed to earth-bound dark matter? *Physical Review D*, 79(2):023505, 2009.

[10] Stephen L. Adler. Modeling the flyby anomalies with dark matter scattering: update with additional data and further predictions. *Physical Review*, 2012.

[11] ME McCulloch. Modelling the flyby anomalies using a modification of inertia. *Monthly Notices of the Royal Astronomical Society: Letters*, 389(1):L57–L60, 2008.

[12] Ignazio Ciufolini and John Archibald Wheeler. *Gravitation and inertia.* Princeton University Press, 1995.

[13] Norman Richard Draper, Harry Smith, and Elizabeth Pownell. *Applied regression analysis*, volume 3. Wiley New York, 1966.

[14] Francis J Anscombe. Graphs in statistical analysis. *The American Statistician*, 27(1):17–21, 1973.

[15] B. Jouannic. *The flyby anomaly: an investigation into potential causes*. MSc thesis, Delft University of Technology, Faculty Aerospace Engineering, 2015.

[16] NASA-JPL. NASA Jet Propulsion Laboratory Horizon software. `http://ssd.jpl.nasa.gov/horizons.cgi`, 2015.

[17] IGRF-12. International Association of Geomagnetism and Aeronomy IGRF model. `http://www.ngdc.noaa.gov/IAGA/vmod/igrf.html`, 2014. Accessed: 2014-11-15.

[18] SILSO. World Data Center for the production, preservation and dissemination of the international sunspot number. `http://www.sidc.be/silso/`, 2015. Accessed: 2014-11-15.

[19] NASA. NASA's Science Mission Directorate. `http://science.nasa.gov/missions/`, 2015. Accessed: 2014-09-15.

[20] ESA. ESA's Science & Technology website. `http://sci.esa.int/home/`, 2015. Accessed: 2014-09-15.

[21] D. Rowlands, J. Marshall, J. McCarthy, D. Moore, D. Pavlis, S. Rowton, S. Luthcke, and L. Tsaoussi. GEODYN II system description. *Hughes-STX Contractor Report*, 1993.

[22] NASA. NASA 3D Models Gallery. `http://www.nasa.gov/multimedia/3d_resources/models.html`, 2013. Accessed: 2013-09-09.

[23] NASA. National Space Science Data Center. `http://nssdc.gsfc.nasa.gov/`, 2014. Accessed: 2014-10-01.

[24] MJ Meshishnek, SR Gyetvay, and CH Jaggers. Long duration exposure facility experiment m0003 deintegration/findings and impacts. In *LDEF, 69 months in space: first post-retrieval symposium*, volume 3134, page 1073, 1991.